Hydrothermal synthesis and crystal structure of poly[bis(μ₃-3,4-diaminobenzoato)manganese], a layered coordination polymer

Muhammad Kaleem Khosa,[a] Paul T. Wood,[b] Simon M. Humphrey[c] and William T. A. Harrison[d]*

[a]Department of Chemistry, Government College University, Faisalabad 38000, Pakistan, [b]Department of Chemistry, University of Cambridge, Lensfield Road, Cambridge CB2 1EW, England, [c]Department of Chemistry and Biochemistry, The University of Texas at Austin, 1 University Station, Austin, Texas 78712, USA, and [d]Department of Chemistry, University of Aberdeen, Meston Walk, Aberdeen AB24 3UE, Scotland. *Correspondence e-mail: w.harrison@abdn.ac.uk

The hydrothermal synthesis and crystal structure of the title two-dimensional coordination polymer, poly[bis(μ₃-3,4-diaminobenzoato-$\kappa^3 N^3,O,O'$)manganese(II)], [Mn(C₇H₇N₂O₂)₂]$_n$, are described. The Mn²⁺ cation (site symmetry $\bar{1}$) adopts a tetragonally elongated *trans*-MnN₂O₄ octahedral coordination geometry and the μ₃-*N,O,O′* ligand (bonding from both carboxylate O atoms and the *meta*-N atom) links the metal ions into infinite (10$\bar{1}$) layers. The packing is consolidated by intra-layer N—H···O and inter-layer N—H···N hydrogen bonds. The structure of the title compound is compared with other complexes containing the C₇H₇N₂O₂⁻ anion and those of the related M(C₈H₈NO₂)₂ (M = Mn, Co, Ni, Zn) family, where C₈H₈NO₂⁻ is the 3-amino-4-methylbenzoate anion.

1. Chemical context

The benzoate anion, C₇H₅O₂⁻, is a classic ligand in coordination chemistry, with over 1500 crystal structures reported in the Cambridge Structural Database (Groom *et al.*, 2016) for complexes of first-row transition metals, which include monodentate (κO), chelating ($\kappa^2 O,O'$) and bridging (μ^2-*O,O′*) modes for the ligand [for ligand bonding-mode notation, see Janicki *et al.* (2017)]. Functionalized benzoate derivatives add further structural variety: for example, –NH₂ substituents at the *ortho*, *meta* and/or *para* positions of the benzene ring can form or accept hydrogen bonds with respect to nearby acceptor or donor groups and/or bond to another metal ion (*i.e.*, as a possible μ^2-*N,O* or μ^3-*N,O,O′* bridging ligand).
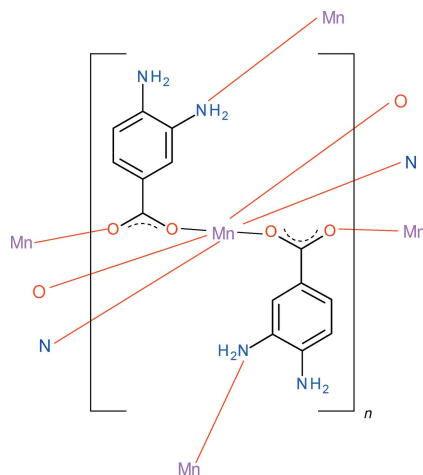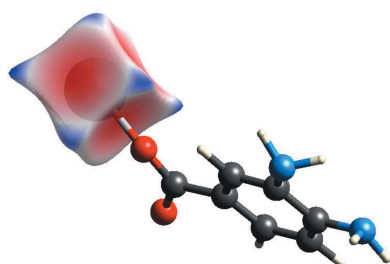
As part of our ongoing studies in this area (Khosa *et al.*, 2015), we now describe the hydrothermal synthesis and crystal structure of the title compound (I), where $C_7H_7N_2O_2{}^-$ is the 3,4-diaminobenzoate (dbz⁻) anion.

2. Structural commentary

The title complex (I) consists of an Mn^{2+} cation located on a crystallographic inversion centre and one deprotonated dbz⁻ ligand with its atoms lying on general positions (Fig. 1), which of course generates the overall 1:2 metal to ligand ratio and ensures charge balance. The C7/O1/O2 carboxylate group of the ligand is rotated from the plane of the C1–C6 aromatic ring by 13.5 (2)° and the C—O bonds [C7—O1 = 1.261 (3) Å and C7—O2 = 1.277 (3) Å] are of similar length, indicating substantial electronic delocalization. The C2—C3 and C5—C6 bonds (mean = 1.383 Å) are marginally shorter than the other bonds in the benzene ring (mean = 1.396 Å), which can be related to resonance of the *para*-N atom lone pair with the carboxylate group (Mukombiwa & Harrison, 2020). This is also presumably reflected in the fact that the C4—N2 bond length [1.413 (3) Å] is slightly shorter than C3—N1 [1.432 (3) Å]. Even so, it is noteworthy that the bond-angle sums about atoms N1 and N2 of 329.8 and 335.8°, respectively, are indicative of a significant tendency towards sp^3 hybridization of the N atoms, *i.e.*, localization of the lone pairs. In terms of the non-hydrogen atoms attached to the benzene ring, N1 and N2 deviate slightly from the mean plane of the ring in opposite directions by −0.023 (3) and 0.024 (3) Å, respectively, whereas atom C7 shows a larger deviation of −0.077 (3) Å.

The dbz⁻ ligand bonds to three different metal ions from both of its carboxylate O atoms and also from its *meta*-N atom (Fig. 1), *i.e.*, $\mu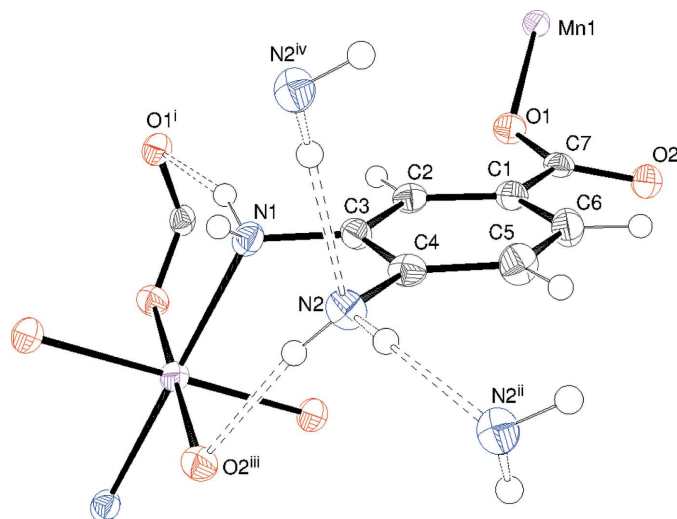^3$-N,O,O′ mode. The preference for the *meta*-N atom to bond to the metal ion (rather than the *para*-N atom) can be related to the resonance effect noted in the previous paragraph. With respect to the carboxylate group, the metal ion bonded to O1 is displaced in an 'upwards' sense by 1.046 (7) Å and the other (bonded to O2) is displaced 'downwards' by −1.651 (6) Å.

Crystal symmetry generates a centrosymmetric *trans*-MnN_2O_4 elongated octahedron for the metal ion, in which the Mn1—N1 bond length of 2.3065 (19) Å is distinctly longer than the Mn1—O1 [2.1591 (14) Å] and Mn1—O2 [2.2062 (15) Å] bonds. The manganese ion presumably has a high-spin $3d^5$ configuration, thus the distortion of the octahedron cannot be electronic in nature (*i.e.*: a Jahn–Teller effect) and might arise for steric reasons. The angular variance (Robinson *et al.*, 1971) of the *cis* X—Mn—Y (X, Y = N, O) bond angles is (7.7°)², indicating relatively little angular distortion from the ideal values of 90°; the minimum and maximum angles are 86.75 (6) and 93.25 (6)°, respectively. The *trans* bond angles are constrained by symmetry to be 180°. The bond-valence sum (in valence units) (Brown & Altermatt, 1985) for the metal ion is 1.97, in very good agreement with the expected value of 2.00 for Mn^{2+}.

In the extended structure of (I), the μ^3 bridging ligand links the metal ions into infinite (10$\bar{1}$) sheets (Fig. 2). These sheets can be decomposed into [010] chains of octahedra linked by the bridging C7/O1/O2 carboxylate groups [shortest Mn···Mn(*x*, *y* + 1, *z*) separation = 4.4212 (2) Å], with connectivity in the [101] direction achieved *via* the benzene ring of the ligands and their *meta*-N atoms [shortest Mn···Mn($-x + \frac{1}{2}$, $y + \frac{1}{2}$, $-z + \frac{1}{2}$) = 8.1520 (4) Å].

Hydrogen bonding helps to consolidate the structure of (I): the *para* –N2H₂ group forms an intra-sheet N2—H4N···O2^{iii} bond (Fig. 1 and Table 1, where symmetry codes are defined) but also participates in an *inter*-sheet N2—H3N···N2^{ii} link, *i.e.*, N2 'accepts its own hydrogen bond' from an adjacent

Figure 1
Fragment of the structure of (I) showing 50% displacement ellipsoids emphasizing the μ^3-N,O,O′ ligand bonding mode and displaying hydrogen bonds as double-dashed lines. [Symmetry codes as in Table 1; additionally: (iv) $-x + \frac{3}{2}$, $y + \frac{1}{2}$, $-z + \frac{1}{2}$.]
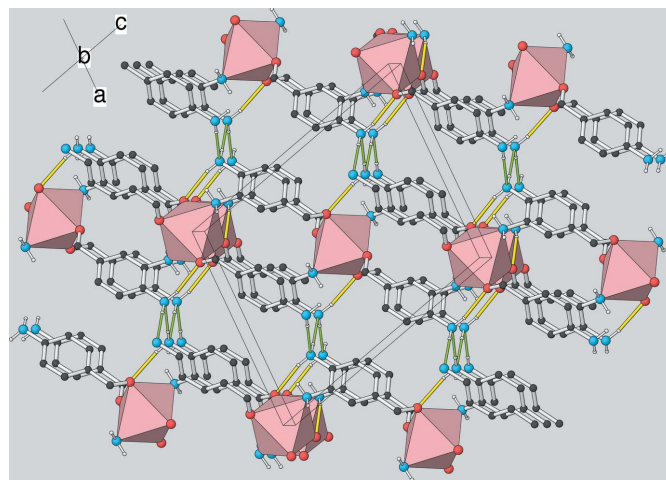

Figure 2
Packing diagram for (I) viewed down [010], showing the (10$\bar{1}$) layers (seen edge-on) with the MnN_2O_4 octahedra shown in polyhedral representation and intralayer N—H···O and interlayer N—H···N hydrogen bonds shown as yellow and green lines, respectively.

Table 1
Hydrogen-bond geometry (Å, °).

D—H$\cdots A$	D—H	H$\cdots A$	$D\cdots A$	D—H$\cdots A$
N1—H1$N\cdots$O1^i	0.88 (3)	2.19 (3)	3.022 (3)	156 (2)
N2—H3$N\cdots$N2^{ii}	0.85 (3)	2.26 (3)	3.106 (3)	178 (2)
N2—H4$N\cdots$O2^{iii}	0.88 (3)	2.15 (3)	3.008 (2)	167 (2)

Symmetry codes: (i) $-x+\frac{1}{2}, y+\frac{1}{2}, -z+\frac{1}{2}$; (ii) $-x+\frac{3}{2}, y-\frac{1}{2}, -z+\frac{1}{2}$; (iii) $x+\frac{1}{2}, -y-\frac{1}{2}, z+\frac{1}{2}$.

Table 2
Hirshfeld surface contact percentages for (I).

H$\cdots$H	33.6
H$\cdots$C	10.2
H$\cdots$O	8.6
H$\cdots$N	2.5
H$\cdots$Mn	0.9
C$\cdots$H	16.1
C$\cdots$C	3.1
O$\cdots$Mn	5.2
O$\cdots$H	10.6
N$\cdots$H	2.5
N$\cdots$Mn	2.0
Mn$\cdots$O	62.0
Mn$\cdots$N	19.3
Mn$\cdots$H	18.8

All contacts are 'non-reciprocal' (*i.e.*, outward facing).

symmetry related –N2H$_2$ group and $C(2)$ infinite chains propagating in the [010] direction arise in the crystal (Figs. 1 and 2) with adjacent N atoms related by the 2_1 screw axis; it is notable that the –NH$_2$ groups in adjacent layers are aligned opposite to each other to facilitate the formation of this inter-sheet hydrogen bond. As well as forming a coordinate bond to the metal ion from N1, the *meta* –N1H$_2$ group forms an N1—H1$N\cdots$O1^i intra-sheet hydrogen bond while the N1—H2N group does not participate in a hydrogen bond, perhaps due to steric crowding. There are no significant aromatic π–π stacking interactions in the crystal of (I), the shortest centroid–centroid separation between C1–C6 rings being 4.4211 (13) Å.

3. Hirshfeld surface analysis

In order to gain further insight into non-covalent interactions in the crystal of (I), the Hirshfeld surface and two-dimensional fingerprint plots were calculated using *CrystalExplorer* (Turner *et al.*, 2017) following the approach recently described by Tan *et al.* (2019). The Hirshfeld surface of the dbz⁻anion in (I) (see supporting information) largely shows the expected red spots of varying intensity corresponding to close contacts resulting from the O—Mn and N—Mn coordinate bonds and N—H$\cdots$O and N—H$\cdots$N hydrogen bonds described above. The Hirshfeld surface mapped onto d_{norm} for the manganese cation in (I) (Fig. 3) is a distinctive 'dimpled cube', with the intense red spots (short interactions) corresponding to its coordinate bonds, which correlates nicely with its octahedral coordination geometry.

The most important outward (*i.e.*, non-reciprocal) percentage contributions of the different type of contacts for the anion and the cation are listed in Table 2. It may be seen that
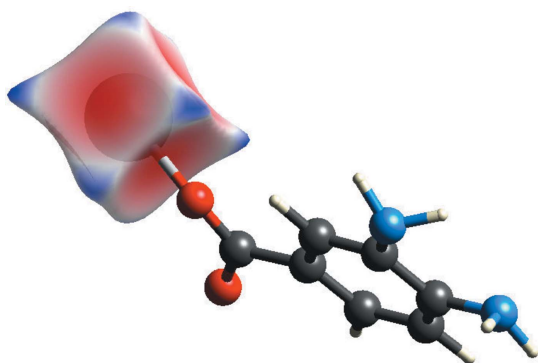
H$\cdots$H (van der Waals) contacts are by far the most significant contributor for the anion followed by C$\cdots$H and H$\cdots$C contacts (total contribution = 59.9%). The contacts associated with the hydrogen bonds, *i.e.*, H$\cdots$N (donor), H$\cdots$O (donor), N$\cdots$H (acceptor) and O$\cdots$H (acceptor) collectively account for some 24.2% of the surface. Finally, the coordinate bonds to the metal ion (O—Mn and N—Mn), despite their presumed importance in establishing the crystal structure, account for a modest 7.2% of the anion's surface.

As might be expected, the Mn—O contacts (62.0%) for the cation dominate its Hirshfeld surface, followed by Mn—N (19.3%), but the ratio of these ($\sim$3.2:1) deviates significantly from the simple 2:1 ratio that would reflect the four Mn—O bonds and two Mn—N bonds. The high percentage of Mn$\cdots$H contacts (18.8%) is notable: these occur at the corners of its cube-like Hirshfeld surface (Fig. 3) and seem to arise from the proximity to the metal ion of the two H atoms attached to N1 [Mn1$\cdots$H1N = 2.58 (3); Mn1$\cdots$H2N = 2.68 (3) Å] and might be repulsive in nature. For further discussion of short metal$\cdots$hydrogen contacts in coordination compounds and their Hirshfeld surfaces, see Pinto *et al.* (2019).
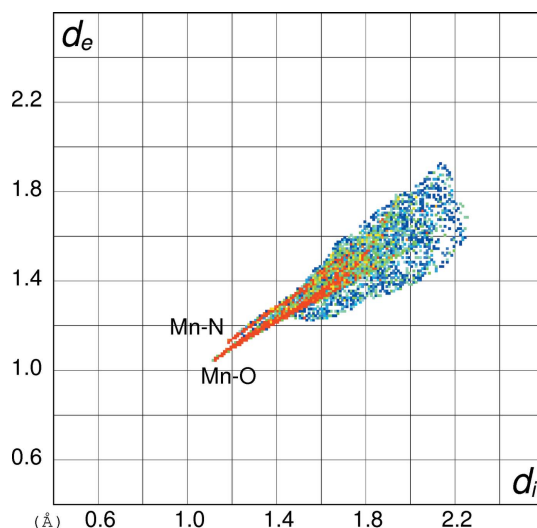

Figure 3
Hirshfeld surface mapped on d_{norm} for the Mn^{2+} cation in (I).

Figure 4
Two-dimensional Hirshfeld fingerprint plot for the Mn^{2+} cation in (I).

Table 3
Structural features of complexes containing the $C_7H_7N_2O_2{}^-$ anion.

Code/refcode	Metal coordination polyhedron	Ligand bonding mode	Topology
(I)	MnN_2O_6 octahedron	μ^3-N,O,O	Layered
BEHJEE	NaO_6 octahedron[a]	κO	Chain
MIWSES	ZnO_3N_2 trigonal bipyramid[a]	μ^2-N,O	Chain
XUPRUV	SnC_3O tetrahedron[b]	κO	Molecular
XUPSAC	SnC_3NO trigonal bipyramid	μ^2-N,O	Chain
YENKOR	NdO_9 capped square antiprism[a]	κO and $\kappa^2 O,O'$	Molecular

Notes: (a) Some of the ligands are water molecules of crystallization; (b) a short 'secondary' Sn···O contact (2.68 Å) is also present.

The wing-like two-dimensional fingerprint plot for the manganese cation in (I) (Fig. 4) shows two prominent features: the spike ending at $(d_i, d_e) = (\sim 1.14, \sim 1.06$ Å) and extending backwards corresponds to the Mn—O coordinate bonds and the (1.18, 1.14 Å) feature just separated from it equates with the Mn—N bonds. The Mn···H contacts are overlapped with the Mn—O and Mn—N contacts in the main body of the 'wing' with the shortest Mn···H contact at about (1.40, 1.25 Å), which correlates well with the short Mn···H contacts noted in the previous paragraph.

4. Database survey

The structure of (I) may firstly be compared with the isostructural $M(C_8H_8NO_2)_2$ family [M = Mn (CCDC refcode ULEZUI) (II), Co (ULIBAU), Ni (ULIBEY) and Zn (ULIBIC)], where $C_8H_8NO_2{}^-$ is the 3-amino-4-methyl-benzoate anion (Khosa *et al.*, 2015). These phases contain μ^3-

Figure 5
Packing diagram (redrawn from Khosa *et al.*, 2015) for (II) viewed down [010], with the MnN_2O_4 octahedra shown in polyhedral representation and N—H···X hydrogen bonds shown as yellow lines. Note how the layers, which propagate parallel to the (100) plane in this setting of the space group, are laterally shifted compared to those in Fig. 2: the shortest inter-layer N···N separation in (I) is 3.106 (3) Å (*via* the N1—H1N···N1 hydrogen bond) compared to the shortest inter-layer C···C separation of 3.948 (2) Å in (II).

Table 4
Experimental details.

Crystal data	
Chemical formula	$[Mn(C_7H_7N_2O_2)_2]$
M_r	357.23
Crystal system, space group	Monoclinic, $P2_1/n$
Temperature (K)	180
a, b, c (Å)	11.5171 (5), 4.4212 (2), 13.9752 (7)
β (°)	104.698 (3)
V (Å^3)	688.32 (6)
Z	2
Radiation type	Mo $K\alpha$
μ (mm^{-1})	0.99
Crystal size (mm)	$0.23 \times 0.10 \times 0.05$
Data collection	
Diffractometer	Nonius KappaCCD
Absorption correction	Multi-scan (*SORTAV*; Blessing, 1995)
T_{min}, T_{max}	0.869, 0.983
No. of measured, independent and observed [$I > 2\sigma(I)$] reflections	5289, 1345, 1105
R_{int}	0.042
$(\sin \theta/\lambda)_{max}$ (Å^{-1})	0.617
Refinement	
$R[F^2 > 2\sigma(F^2)]$, $wR(F^2)$, S	0.031, 0.074, 1.05
No. of reflections	1345
No. of parameters	119
H-atom treatment	H atoms treated by a mixture of independent and constrained refinement
$\Delta\rho_{max}$, $\Delta\rho_{min}$ (e Å^{-3})	0.27, −0.28

Computer programs: *COLLECT* (Nonius, 1998), *HKL DENZO* and *SCALEPACK* (Otwinowski & Minor, 1997), *SORTAV* (Blessing, 1995), *SHELXS97* (Sheldrick, 2008), *SHELXL2014/7* (Sheldrick, 2015), *ORTEP-3 for Windows* (Farrugia, 2012), *ATOMS* (Shape Software, 2007) and *publCIF* (Westrip, 2010).

N,O,O' ligands and centrosymmetric MN_2O_4 octahedra, which generate very similar polymeric layers to those found in (I). In (II), the sheets propagate parallel to the (100) plane of the monoclinic cell due to a different choice of unit-cell setting (see *Refinement* section). The major difference arises with respect to the *para*-substituent: in (II) the methyl groups in adjacent (100) layers are laterally shifted with respect to each other (Fig. 5) to avoid an unfavourable close steric contact and there are no directional inter-sheet interactions beyond normal van der Waals' contacts, which compares to the inter-layer N—H···N links already mentioned for (I).

Despite its potential as a polyfunctional bridging ligand, just five crystal structures of complexes of the 3,4-diamino-benzoate anion are reported in the Cambridge Structural Database as of March 2020 with sodium (BEHJEE: Rzaczyńska *et al.*, 2003), zinc (MIWSES; Fernández-Palacio *et al.*, 2014), tin (XUPRUV and XUPSAC; Pruchnik *et al.*, 2002) and neodymium (YENKOR; Rzaczyńska *et al.*, 1994). Key data for (I) and these structures are summarized in Table 3, which indicates a wide variety of metal coordination polyhedra, ligand bonding modes and topologies. Unlike the isostructural manganese and zinc phases in the $M(C_8H_8NO_2)_2$ family, MIWSES features a water molecule bonded to the trigonal–bipyramidally coordinated zinc ion and has a quite different overall structure to (I). It may finally be noted that (I)
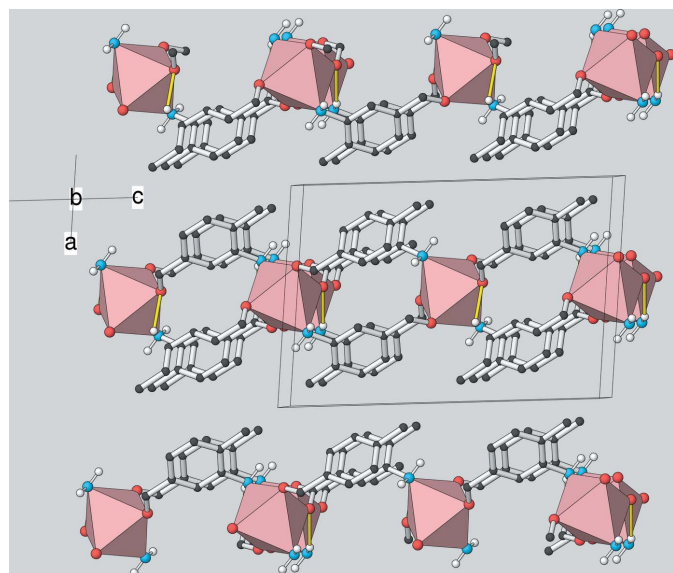
represents the first reported example of a μ^3-N,O,O' bonding mode for the dbz$^-$ anion.

5. Synthesis and crystallization

A mixture of 99 mg (0.50 mmol) of MnCl$_2$·4H$_2$O and 152 mg (1.00 mmol) of 3,4-diaminobenzoic acid were added to 1.0 ml of 1 *M* KOH under stirring. The resulting mixture was heated to 423 K in a 23 ml Teflon-lined autoclave for 10 h. The autoclave was then removed from the oven and cooled to room temperature over several hours and opened. Colourless plates of (I) were recovered by vacuum filtration and rinsed with acetone and dried.

6. Refinement

Crystal data, data collection and structure refinement details are summarized in Table 4. The N-bound H atoms were located in difference maps and their positions were freely refined. The C-bound H atoms were geometrically placed (C—H = 0.95 Å) and refined as riding atoms. The constraint $U_{iso}(H) = 1.2U_{eq}$(carrier) was applied in all cases. The standard setting of the unit cell for (I) (*i.e.*, space group $P2_1/c$) in which the polymeric layers would propagate in the (100) plane, as also found for compound (II), has a = 13.975, b = 4.421, c = 15.693 Å and β = 134.77°, but $P2_1/n$ was chosen here to avoid refinement problems associated with the very obtuse β angle: compare Feast *et al.* (2009).

References

Blessing, R. H. (1995). *Acta Cryst.* A**51**, 33–38.
Brown, I. D. & Altermatt, D. (1985). *Acta Cryst.* B**41**, 244–247.
Farrugia, L. J. (2012). *J. Appl. Cryst.* **45**, 849–854.
Feast, G. C., Haestier, J., Page, L. W., Robertson, J., Thompson, A. L. & Watkin, D. J. (2009). *Acta Cryst.* C**65**, o635–o638.
Fernández-Palacio, F., Restrepo, J., Gálvez, S., Gómez-Sal, P. & Mosquera, M. E. G. (2014). *CrystEngComm*, **16**, 3376–3386.
Groom, C. R., Bruno, I. J., Lightfoot, M. P. & Ward, S. C. (2016). *Acta Cryst.* B**72**, 171–179.
Janicki, R., Mondry, A. & Starynowicz, P. (2017). *Coord. Chem. Rev.* **340**, 98–133.
Khosa, M. K., Wood, P. T., Humphreys, S. M. & Harrison, W. T. A. (2015). *J. Struct. Chem.* **56**, 1130–1135.
Mukombiwa, E. T. & Harrison, W. T. A. (2020). *Acta Cryst.* E**76**, 527–533.
Nonius (1998). *COLLECT* data collection software. Nonius BV, Delft, The Netherlands.
Otwinowski, Z. & Minor, W. (1997). *Methods in Enzymology*, Vol. 276, *Macromolecular Crystallography*, Part A, edited by C. W. Carter Jr & R. M. Sweet, pp. 307–326. New York: Academic Press.
Pinto, C. B., Dos Santos, L. H. R. & Rodrigues, B. L. (2019). *Acta Cryst.* C**75**, 707–716.
Pruchnik, F. P., Bańbuła, M., Ciunik, Z., Chojnacki, H., Latocha, M., Skop, B., Wilczok, T., Opolski, A., Wietrzyk, J. & Nasulewicz, A. (2002). *Eur. J. Inorg. Chem.* pp. 3214–3221.
Robinson, K., Gibbs, G. V. & Ribbe, P. H. (1971). *Science*, **172**, 567–570.
Rzaczyńska, Z., Bartyzel, A. & Głowiak, T. (2003). *J. Coord. Chem.* **56**, 77–83.
Rzaczyńska, Z., Belskii, V. K. & Zavodnik, V. E. (1994). *Pol. J. Chem.* **68**, 1639–1647.
Shape Software (2007). *ATOMS*. Shape Software, Kingsport, Tennessee, USA.
Sheldrick, G. M. (2008). *Acta Cryst.* A**64**, 112–122.
Sheldrick, G. M. (2015). *Acta Cryst.* C**71**, 3–8.
Tan, S. L., Jotani, M. M. & Tiekink, E. R. T. (2019). *Acta Cryst.* E**75**, 308–318.
Turner, M. J., McKinnon, J. J., Wolff, S. K., Grimwood, D. J., Spackman, P. R., Jayatilaka, D. & Spackman, M. A. (2017). *CrystalExplorer17*. University of Western Australia. http://hirshfeldsurface.net
Westrip, S. P. (2010). *J. Appl. Cryst.* **43**, 920–925.

Hydrothermal synthesis and crystal structure of poly[bis(μ_3-3,4-diamino-benzoato)manganese], a layered coordination polymer

Muhammad Kaleem Khosa, Paul T. Wood, Simon M. Humphrey and William T. A. Harrison

Computing details

Data collection: *COLLECT* (Nonius, 1998); cell refinement: *HKL SCALEPACK* (Otwinowski & Minor, 1997); data reduction: *HKL DENZO* and *SCALEPACK* (Otwinowski & Minor, 1997), *SORTAV* (Blessing, 1995); program(s) used to solve structure: *SHELXS97* (Sheldrick, 2008); program(s) used to refine structure: *SHELXL2014/7* (Sheldrick, 2015); molecular graphics: *ORTEP-3 for Windows* (Farrugia, 2012) and *ATOMS* (Shape Software, 2007); software used to prepare material for publication: *publCIF* (Westrip, 2010).

Poly[bis(μ_3-3,4-diaminobenzoato-κ^3N^3,O,O')manganese(II)]

Crystal data

[Mn(C$_7$H$_7$N$_2$O$_2$)$_2$]	$F(000) = 366$
$M_r = 357.23$	$D_x = 1.724$ Mg m^{-3}
Monoclinic, $P2_1/n$	Mo $K\alpha$ radiation, $\lambda = 0.71073$ Å
$a = 11.5171$ (5) Å	Cell parameters from 5315 reflections
$b = 4.4212$ (2) Å	$\theta = 1.0$–26.0°
$c = 13.9752$ (7) Å	$\mu = 0.99$ mm^{-1}
$\beta = 104.698$ (3)°	$T = 180$ K
$V = 688.32$ (6) Å^3	Slab, colourless
$Z = 2$	$0.23 \times 0.10 \times 0.05$ mm

Data collection

Nonius KappaCCD diffractometer	1345 independent reflections
	1105 reflections with $I > 2\sigma(I)$
ω and φ scans	$R_{int} = 0.042$
Absorption correction: multi-scan (*SORTAV*; Blessing, 1995)	$\theta_{max} = 26.0°$, $\theta_{min} = 2.1°$
$T_{min} = 0.869$, $T_{max} = 0.983$	$h = -14 \rightarrow 13$
	$k = -5 \rightarrow 5$
5289 measured reflections	$l = -17 \rightarrow 17$

Refinement

Refinement on F^2	Primary atom site location: structure-invariant direct methods
Least-squares matrix: full	
$R[F^2 > 2\sigma(F^2)] = 0.031$	Hydrogen site location: mixed
$wR(F^2) = 0.074$	H atoms treated by a mixture of independent and constrained refinement
$S = 1.05$	
1345 reflections	$w = 1/[\sigma^2(F_o^2) + (0.0282P)^2 + 0.509P]$ where $P = (F_o^2 + 2F_c^2)/3$
119 parameters	
0 restraints	$(\Delta/\sigma)_{max} < 0.001$
	$\Delta\rho_{max} = 0.27$ e Å^{-3}

$\Delta\rho_{min} = -0.28$ e Å^{-3}

Extinction correction: SHELXL2018/3 (Sheldrick 2015), $Fc^* = kFc[1+0.001xFc^2\lambda^3/\sin(2\theta)]^{-1/4}$
Extinction coefficient: 0.012 (2)

Special details

Geometry. All esds (except the esd in the dihedral angle between two l.s. planes) are estimated using the full covariance matrix. The cell esds are taken into account individually in the estimation of esds in distances, angles and torsion angles; correlations between esds in cell parameters are only used when they are defined by crystal symmetry. An approximate (isotropic) treatment of cell esds is used for estimating esds involving l.s. planes.

Fractional atomic coordinates and isotropic or equivalent isotropic displacement parameters (Å^2)

	x	*y*	*z*	U_{iso}*/U_{eq}
Mn1	0.000000	0.500000	0.000000	0.01883 (17)
C1	0.32186 (18)	−0.0488 (5)	0.11717 (15)	0.0195 (5)
C2	0.36414 (18)	0.1055 (5)	0.20598 (15)	0.0198 (5)
H2	0.312438	0.241153	0.228031	0.024*
C3	0.48037 (18)	0.0642 (5)	0.26264 (15)	0.0192 (5)
C4	0.55799 (18)	−0.1335 (5)	0.23063 (16)	0.0204 (5)
C5	0.51634 (19)	−0.2802 (5)	0.13985 (17)	0.0254 (5)
H5	0.568982	−0.407707	0.115733	0.030*
C6	0.39925 (19)	−0.2419 (5)	0.08470 (16)	0.0242 (5)
H6	0.371484	−0.348284	0.024144	0.029*
C7	0.19402 (18)	−0.0122 (5)	0.06079 (14)	0.0181 (4)
N1	0.52161 (17)	0.2169 (4)	0.35541 (13)	0.0205 (4)
H1N	0.482 (2)	0.387 (6)	0.3585 (18)	0.025*
H2N	0.596 (2)	0.262 (6)	0.3646 (18)	0.025*
N2	0.67763 (16)	−0.1663 (5)	0.28747 (15)	0.0229 (4)
H3N	0.716 (2)	−0.306 (6)	0.2669 (18)	0.028*
H4N	0.681 (2)	−0.190 (6)	0.350 (2)	0.028*
O1	0.13370 (12)	0.1975 (3)	0.08586 (11)	0.0224 (4)
O2	0.15011 (13)	−0.1998 (3)	−0.00841 (11)	0.0229 (4)

Atomic displacement parameters (Å^2)

	U^{11}	U^{22}	U^{33}	U^{12}	U^{13}	U^{23}
Mn1	0.0190 (3)	0.0173 (3)	0.0187 (3)	0.00075 (19)	0.00188 (18)	0.00021 (19)
C1	0.0194 (10)	0.0188 (12)	0.0196 (10)	−0.0010 (8)	0.0034 (9)	0.0023 (8)
C2	0.0198 (10)	0.0176 (11)	0.0225 (11)	0.0022 (8)	0.0064 (9)	0.0021 (9)
C3	0.0198 (10)	0.0200 (12)	0.0171 (10)	−0.0027 (8)	0.0033 (8)	0.0013 (8)
C4	0.0165 (10)	0.0203 (11)	0.0238 (11)	−0.0015 (9)	0.0041 (9)	0.0039 (9)
C5	0.0233 (11)	0.0276 (13)	0.0265 (12)	0.0059 (10)	0.0088 (9)	−0.0022 (10)
C6	0.0258 (11)	0.0256 (12)	0.0201 (11)	0.0009 (10)	0.0036 (9)	−0.0028 (9)
C7	0.0198 (10)	0.0176 (10)	0.0168 (10)	−0.0030 (9)	0.0044 (8)	0.0042 (9)
N1	0.0189 (9)	0.0182 (10)	0.0230 (9)	−0.0018 (8)	0.0027 (8)	−0.0021 (8)
N2	0.0185 (9)	0.0273 (11)	0.0232 (10)	0.0037 (8)	0.0058 (8)	0.0013 (9)
O1	0.0208 (8)	0.0215 (8)	0.0234 (8)	0.0047 (6)	0.0026 (6)	0.0013 (6)
O2	0.0227 (8)	0.0232 (8)	0.0215 (8)	−0.0022 (6)	0.0031 (6)	−0.0017 (7)

Geometric parameters (Å, º)

Mn1—O1	2.1591 (14)	C3—N1	1.432 (3)
Mn1—O1ⁱ	2.1591 (14)	C4—C5	1.397 (3)
Mn1—O2ⁱⁱ	2.2062 (15)	C4—N2	1.413 (3)
Mn1—O2ⁱⁱⁱ	2.2062 (15)	C5—C6	1.383 (3)
Mn1—N1^{iv}	2.3065 (19)	C5—H5	0.9500
Mn1—N1^v	2.3065 (19)	C6—H6	0.9500
C1—C6	1.391 (3)	C7—O1	1.261 (3)
C1—C2	1.392 (3)	C7—O2	1.277 (3)
C1—C7	1.492 (3)	N1—H1N	0.88 (3)
C2—C3	1.384 (3)	N1—H2N	0.86 (3)
C2—H2	0.9500	N2—H3N	0.85 (3)
C3—C4	1.402 (3)	N2—H4N	0.88 (3)
O1—Mn1—O1ⁱ	180.0	C5—C4—C3	118.65 (19)
O1—Mn1—O2ⁱⁱ	93.20 (6)	C5—C4—N2	121.6 (2)
O1ⁱ—Mn1—O2ⁱⁱ	86.80 (6)	C3—C4—N2	119.64 (19)
O1—Mn1—O2ⁱⁱⁱ	86.80 (6)	C6—C5—C4	120.7 (2)
O1ⁱ—Mn1—O2ⁱⁱⁱ	93.20 (6)	C6—C5—H5	119.7
O2ⁱⁱ—Mn1—O2ⁱⁱⁱ	180.0	C4—C5—H5	119.7
O1—Mn1—N1^{iv}	90.52 (6)	C5—C6—C1	120.6 (2)
O1ⁱ—Mn1—N1^{iv}	89.48 (6)	C5—C6—H6	119.7
O2ⁱⁱ—Mn1—N1^{iv}	93.25 (6)	C1—C6—H6	119.7
O2ⁱⁱⁱ—Mn1—N1^{iv}	86.75 (6)	O1—C7—O2	123.23 (18)
O1—Mn1—N1^v	89.48 (6)	O1—C7—C1	118.20 (18)
O1ⁱ—Mn1—N1^v	90.52 (6)	O2—C7—C1	118.53 (19)
O2ⁱⁱ—Mn1—N1^v	86.75 (6)	C3—N1—Mn1^{vi}	120.83 (14)
O2ⁱⁱⁱ—Mn1—N1^v	93.25 (6)	C3—N1—H1N	112.9 (16)
N1^{iv}—Mn1—N1^v	180.0	Mn1^{vi}—N1—H1N	98.0 (16)
C6—C1—C2	118.93 (19)	C3—N1—H2N	109.6 (17)
C6—C1—C7	121.50 (18)	Mn1^{vi}—N1—H2N	107.0 (17)
C2—C1—C7	119.54 (19)	H1N—N1—H2N	107 (2)
C3—C2—C1	121.0 (2)	C4—N2—H3N	113.5 (17)
C3—C2—H2	119.5	C4—N2—H4N	111.1 (16)
C1—C2—H2	119.5	H3N—N2—H4N	111 (2)
C2—C3—C4	120.14 (19)	C7—O1—Mn1	131.83 (13)
C2—C3—N1	120.44 (19)	C7—O2—Mn1^{vii}	121.03 (13)
C4—C3—N1	119.41 (18)		
C6—C1—C2—C3	−1.4 (3)	C7—C1—C6—C5	−177.8 (2)
C7—C1—C2—C3	176.57 (19)	C6—C1—C7—O1	−169.7 (2)
C1—C2—C3—C4	0.5 (3)	C2—C1—C7—O1	12.4 (3)
C1—C2—C3—N1	−178.0 (2)	C6—C1—C7—O2	12.3 (3)
C2—C3—C4—C5	1.6 (3)	C2—C1—C7—O2	−165.55 (19)
N1—C3—C4—C5	−179.9 (2)	C2—C3—N1—Mn1^{vi}	89.4 (2)
C2—C3—C4—N2	177.9 (2)	C4—C3—N1—Mn1^{vi}	−89.1 (2)
N1—C3—C4—N2	−3.5 (3)	O2—C7—O1—Mn1	−40.5 (3)

C3—C4—C5—C6	−2.9 (3)	C1—C7—O1—Mn1	141.59 (15)
N2—C4—C5—C6	−179.1 (2)	O1—C7—O2—Mn1[vii]	−60.8 (2)
C4—C5—C6—C1	2.0 (3)	C1—C7—O2—Mn1[vii]	117.02 (17)
C2—C1—C6—C5	0.1 (3)		

Symmetry codes: (i) −x, −y+1, −z; (ii) −x, −y, −z; (iii) x, y+1, z; (iv) x−1/2, −y+1/2, z−1/2; (v) −x+1/2, y+1/2, −z+1/2; (vi) −x+1/2, y−1/2, −z+1/2; (vii) x, y−1, z.

Hydrogen-bond geometry (Å, °)

D—H···A	D—H	H···A	D···A	D—H···A
N1—H1N···O1[v]	0.88 (3)	2.19 (3)	3.022 (3)	156 (2)
N2—H3N···N2[viii]	0.85 (3)	2.26 (3)	3.106 (3)	178 (2)
N2—H4N···O2[ix]	0.88 (3)	2.15 (3)	3.008 (2)	167 (2)

Symmetry codes: (v) −x+1/2, y+1/2, −z+1/2; (viii) −x+3/2, y−1/2, −z+1/2; (ix) x+1/2, −y−1/2, z+1/2.